Vascular CD39/ENTPD1 Directly Promotes Tumor Cell Growth by Scavenging Extracellular Adenosine Triphosphate[1,2]

Lili Feng[*,†,3], Xiaofeng Sun[*,3], Eva Csizmadia[*], Lihui Han[*], Shu Bian[*], Takashi Murakami[‡], Xin Wang[†], Simon C. Robson[*,4] and Yan Wu[*,4]

*Department of Medicine, Transplantation Institute, Beth Israel Deaconess Medical Center, Harvard Medical School, Boston, MA, USA; †Department of Hematology, Provincial Hospital Affiliated to Shandong University, Jinan, PR China; ‡Division of Bioimaging Sciences, Center for Molecular Medicine, Jichi Medical University, Shimotsuke, Tochigi, Japan

Abstract

Extracellular adenosine triphosphate (ATP) is known to boost immune responses in the tumor microenvironment but might also contribute directly to cancer cell death. CD39/ENTPD1 is the dominant ectonucleotidase expressed by endothelial cells and regulatory T cells and catalyzes the sequential hydrolysis of ATP to AMP that is further degraded to adenosine by CD73/ecto-5′-nucleotidase. We have previously shown that deletion of *Cd39* results in decreased growth of transplanted tumors in mice, as a result of both defective angiogenesis and heightened innate immune responses (secondary to loss of adenosinergic immune suppression). Whether alterations in local extracellular ATP and adenosine levels as a result of CD39 bioactivity directly affect tumor growth and cytotoxicity has not been investigated to date. We show here that extracellular ATP exerts antitumor activity by directly inhibiting cell proliferation and promoting cancer cell death. ATP-induced antiproliferative effects and cell death are, in large part, mediated through P2X$_7$ receptor signaling. Tumors in *Cd39* null mice exhibit increased necrosis in association with P2X$_7$ expression. We further demonstrate that exogenous soluble NTPDase, or CD39 expression by cocultured liver sinusoidal endothelial cells, stimulates tumor cell proliferation and limits cell death triggered by extracellular ATP. Collectively, our findings indicate that local expression of CD39 directly promotes tumor cell growth by scavenging extracellular ATP. Pharmacological or targeted inhibition of CD39 enzymatic activity may find utility as an adjunct therapy in cancer management.

Neoplasia (2011) 13, 206–216

Introduction

Adenosine triphosphate (ATP) mediates multiple physiological reactions and plays a crucial role in cellular metabolism, inclusive of roles in bioenergetics [1–3]. Extracellular ATP acts on type 2 purinergic (P2) receptors to exert signaling effects. There are two P2 families: seven P2X ion channel receptors recognizing ATP (P2X$_{1-7}$) and eight P2Y G protein–coupled receptors (P2Y$_{1, 2, 4, 6, 11-14}$) that bind several nucleoside triphosphates and diphosphates [4–6]. Documented cytotoxic effects of extracellular ATP on various malignant cells have elicited attention to this signaling pathway [2,7–10]. Five P2 receptor subtypes have been considered to be involved in the antitumor actions of ATP, namely P2X$_5$, P2X$_7$, P2Y$_1$, P2Y$_2$, and P2Y$_{11}$ (exclusively in human), but precise roles for these receptors are not well defined [2,9,11].

Intracellular ATP concentrations are typically of the order of 3 to 10 mM. Basal concentrations of extracellular ATP, in contrast, are considered to be around 10 nM. The latter levels are maintained by ectonucleotidases, which hydrolyze released ATP sequentially to adenosine diphosphate (ADP), adenosine monophosphate (AMP), and further to adenosine [12]. These ectoenzymes result in a 10^6-fold gradient for potential ATP efflux. Therefore, the release of a small amount of intracellular ATP could elicit a dramatic elevation of extracellular ATP concentration thereby affecting purinergic signaling [13].

Anticancer chemotherapies directly induce tumor cell death. Dying tumor cells release mediators that signal cellular damage (e.g., uric acid, nucleic acids, alum, high mobility group box 1 protein) [14,15]. These signals may be recognized by dendritic cells, which further provoke anticancer immune responses [16–18]. ATP has been recently identified as a novel danger signal emitted by dying tumor cells and is also released by immune cells. ATP is considered important for the efficient immune responses required for the successful anticancer therapies [19]. ATP can also be released from the cytosol of necrotic cells, which are always present in the center of fast-growing tumors [11], such as in transplanted melanomas [20,21].

CD39/ENTPD1 (ectonucleoside triphosphate diphosphohydrolase 1) is the dominant ectonucleotidase expressed by endothelial cells (ECs) and regulatory T cells (Treg) [22–24]. We have previously demonstrated that deletion of *Cd39* results in reduction of melanoma growth and inhibition of pulmonary metastases, associated with abrogation of angiogenesis [20]. We have also recently shown that CD39 expression on Treg inhibits NK cell–mediated antitumor activity and is permissive for hepatic metastatic tumor growth, whereas vascular CD39 boosts angiogenesis [21]. When ATP appears in the extracellular space of tumor microenvironment, it is quickly metabolized by CD39 to AMP. Therefore, in *Cd39* null mice, failure of removal of ATP released by necrotic tumor cells in the center of fast-growing tumors might cause acute increases in levels of local extracellular ATP and result in killing of adjacent tumor cells.

Given that CD39 has been implicated in promoting tumor growth and metastases through the suppression of antitumor immune responses and enhancement of angiogenesis [20,21], we further hypothesized that CD39 expression by ECs might directly protect tumor cells from high levels of extracellular ATP (from whatever source). In this study, we demonstrate that extracellular ATP directly limits tumor cell growth and that these antitumor effects could be mitigated by provision of CD39/apyrase or by the intrinsic EC expression of CD39. Targeting the expression and/or ectoenzymatic activity of CD39 in combination with other chemotherapy regimens might provide a novel approach to cancer therapy.

Materials and Methods

Mice

Eight- to twelve-week-old male *Cd39* null and *Cd73* null mice on the C57BL/6 background (have been interbred and backcrossed ×12) were used [23,25]. Age-, sex-, and strain-matched wild-type mice were purchased from Taconic (Hudson, NY). All experimental mice were kept in a temperature-controlled room with alternating 12-hour dark-light cycles. Animal experimentation protocols were reviewed and approved by the Institutional Animal Care and Use Committees of Beth Israel Deaconess Medical Center.

Tumor Cell Lines

Luciferase-expressing B16/F10 (luc-B16/F10), a genetically modified C57BL/6 mouse melanoma cell line, was established as previously described [26]. Syngeneic C57BL/6 murine MCA38 colon cancer cells were provided by Dr Nicholas P. Restifo (National Cancer Institute). All cell lines were tested for *Mycoplasma* and other infections by mouse IMPACT III PCR Profile using RADIL (Columbia, MO) and were maintained as described previously [21].

Antibodies and Reagents

Rabbit anti-P2X$_7$ antibody was purchased from Alomone Laboratories (Jerusalem, Israel) [27,28]. Mouse anti–β-actin monoclonal antibody was from Abcam (Cambridge, MA). The rabbit antibodies against cleaved caspase-3 (Asp175), cleaved caspase-9 (Asp353), caspase-3 (8G10), and caspase-9 were purchased from Cell Signaling Technology (Danvers, MA). Rat anti–mouse CD31 antibody was obtained from R&D Systems (Minneapolis, MN). The production of rabbit polyclonal anti–mouse CD39 antibody (C9F) has been described previously [29]. ^{3}H-thymidine was purchased from Perkin-Elmer (Waltham, MA). All chemicals were obtained from Sigma-Aldrich (St Louis, MO), unless otherwise stated.

Assessment of Cell Proliferation and Cell Viability

Cells (5×10^3) were seeded into 96-well plates and cultured for 24 hours. Nucleotides were then added into cultures. Sixteen hours later, cell viability was analyzed using Cell Counting Kit-8 (Dojindo Molecular Technologies, Inc, Rockville, MD) following the manufacturer's instructions. In parallel, ^{3}H-thymidine (1 μCi/well) was added into the cultures immediately after addition of nucleotides, and cell proliferation was evaluated 16 hours later using ^{3}H-TdR incorporation method as described previously [30].

In Situ Cellular Analysis

Cells (5×10^3) were seeded into Corning 3603 Black 96-well plates and cultured for 24 hours before being exposed to ATP. Sixteen hours later, cell growth was evaluated using the Celigo Cytometer (Cyntellect, Inc, San Diego, CA). Cells were imaged and counted using the Celigo Cell Counting application.

Liver Sinusoidal Endothelial Cell Culture

Liver sinusoidal endothelial cells (LSECs) were isolated, and cell purity was assayed using acetylated low-density lipoprotein labeled with 1,1′-dioctadecyl-3,3,3′3′-tetramethylindo-carbocyanine perchlorate (10 μg/ml) following the manufacturer's instructions (Biomedical Technologies, Inc, Stoughton, MA) as previously described [31,32]. The purity of LSECs was greater than 99%.

Cotreatment or Coculture Experiments

For experiments with apyrase or antagonist treatment, luc-B16/F10 cells were pretreated with apyrase, KN-62 (Tocris Bioscience, Ellisville, MO), MRS-2500, or suramin for 30 minutes before being exposed to treatment of ATP. For coculture experiments, LSECs were seeded together with luc-B16/F10 cells (3×10^3) at indicated ratios of cell numbers into fibronectin-coated plates and cultured in 1:1 mixtures of LSEC medium and luc-B16/F10 medium for 24 hours before being exposed to further treatments.

Immunoblot Analysis

Cultured cells were lysed in modified RIPA buffer containing 50 mM Tris-HCl (pH 7.4), 150 mM NaCl, 0.5% sodium deoxycholate, 0.1% SDS, 1% NP-40, phosphatase inhibitors (Sigma-Aldrich), and protease inhibitor cocktail tablets (Roche Applied Science, Mannheim, Germany). The measurement of protein concentrations and detailed procedures of immunoblot analysis were described previously [33].

Reverse Transcription–Polymerase Chain Reaction and Real-time Quantitative PCR

Total RNA were extracted and purified from cells using an RNeasy kit (Qiagen, Valencia, CA). Reverse transcription was conducted on 1 μg of total RNA using ABI Prism TaqMan reverse transcription reagents (Applied Biosystems, Foster City, CA). Reverse transcription–polymerase chain reaction (RT-PCR) and real-time quantitative PCR (RQ-PCR) analyses were performed as described previously [33,34]. Specific primers for RT-PCR were obtained from Invitrogen (Carlsbad, CA), and the primer sequences were shown in Table W1. Primer probe sets of $P2X_7$ and GAPDH used for RQ-PCR were purchased from Applied Biosystems.

Flow Cytometric Analysis

After treatment of luc-B16/F10 cells with ATP or together with KN-62 for the indicated periods, apoptotic cells and necrotic cells were analyzed by staining the cells with fluorescein isothiocyanate (FITC)–annexin V and propidium iodide (PI), according to the manufacturer's instructions (apoptosis kit; BD Pharmingen, San Diego, CA). Briefly, an aliquot of 10^5 cells was incubated with FITC–annexin V and PI for 15 minutes at room temperature in the dark. Cells were then immediately analyzed by LSR II (BD Biosciences). Viable cells are not stained with FITC–annexin V or PI. The necrotic cells were FITC–annexin V and PI-positive, whereas apoptotic cells were annexin V–positive and PI-negative [35,36]. FACS data were analyzed using FlowJo software (TreeStar, Inc, Ashland, OR).

Tumor Supernatant Preparation

Luc-B16/F10 cells (5×10^5) were injected (s.c.) into flanks of wild-type C57BL/6 mice as previously established [20]. On day 14, tumors were separated, weighed, excised, and washed once with complete RPMI 1640 medium. Media were collected as "prewash" media. The tumor tissues supplemented with fresh media were then passed through a 100-μm cell strainer. The filtrates were then subjected to snap-freeze (in liquid nitrogen)–thaw cycles (twice to disrupt cell membranes), followed by centrifugation at 14,000 rpm for 30 minutes at 4°C. Supernatants were collected as "tumor supernatants" and immediately added into luc-B16/F10 cell cultures.

Measurement of ATP Levels in Biologic Samples

The "prewash" media and "tumor supernatants" were subjected to a deproteinizing sample preparation kit (BioVision, Mountain View, CA) to remove the proteins, followed by assays of ATP levels using the ATP Colorimetric/Fluorometric Assay Kit (BioVision) in accordance with the manufacturer's instructions.

Hepatic Metastatic Melanoma Model

This was preformed as described previously [21]. Briefly, luc-B16/F10 cells (2×10^5) were infused into liver through portal vein of C57BL/6 mice. After 14 days, the mice were killed and examined for tumor growth in the liver.

Immunocytohistochemistry and Immunofluorescence

These procedures were performed as previously [20,21,33,37]. Luc-B16/F10 cells (1×10^3) were seeded on poly-D-lysine/laminin–coated glass coverslips (BD Biosciences) and cultured for 4 days before being exposed to treatment.

Thin-Layer Chromatography Analysis

Enzymatic activity of freshly isolated LSECs or luc-B16/F10 cells was analyzed using thin-layer chromatography (TLC), as previously described [30,34]. A total of 3×10^5 cells were analyzed.

Statistical Analysis

All data are represented as means ± SD of values (obtained from at least three independent experiments in triplicates). All histologic and immunohistochemical images are representative of at least four mice per group. All statistical analyses were performed using the 2-tailed Student's t test. Significance was defined as $P < .05$.

Results

Antiproliferative Functions of ATP Are Mediated through $P2X_7$ Receptor

Luc-B16/F10 cells were used for the present study. We first examined the effects of extracellular ATP at high concentrations on the proliferation of these B16 melanoma cells. As shown in Figure 1A, cell proliferation was inhibited by exposure (16 hours) of ATP in a concentration-dependent manner. BzATP (synthetic nonhydrolyzable and potent ATP analogue) had more potent inhibitory effects on melanoma cell proliferation (Figure 1B), as expected. Similar inhibitory effects of extracellular ATP on other MCA38 colon cancer cells were also observed, albeit with differential dose-response curves (Figure W1).

To investigate involvement of P2 receptor(s) in the effects on ATP-induced proliferation, we first examined mRNA expression of all P2 receptors by RT-PCR analysis using total RNA from luc-B16/F10 cells (Figure 1C). Luc-B16/F10 cells expressed mRNA of several P2 receptors but not $P2X_6$, $P2Y_4$, and $P2Y_{11}$.

It has been recently reported that $P2X_7$ and $P2Y_1$ might be the major P2 receptors responsible for the antimelanoma activity of ATP in human cells [38]. Next, therefore luc-B16/F10 cells were incubated with P2 antagonists including KN-62 (to $P2X_7$), MRS-2500 (to $P2Y_1$), and suramin (nonselective to P2Rs), together with ATP (2.5 mM) for 16 hours. Changes in cell proliferation were then evaluated. Coincubation of cells with KN-62 decreased the extent of ATP-induced inhibition on melanoma cell proliferation in a dose-dependent manner (60% at 1 μM and 70% at 2.5 μM) with noted cytotoxicity of 2.5 μM KN-62 alone (Figure 1D). MRS-2500 (Figure 1E), or suramin (data not shown), failed to block the inhibitory effects of ATP.

We next performed Western blot analysis using total cell lysates from luc-B16/F10 cells to examine the protein expression of $P2X_7$ in these cells. For comparison, a human embryonic kidney (HEK293) cells line, which does not express $P2X_7$ [39], was also tested as a negative control. As shown in Figure 1F, $P2X_7$ was expressed in luc-B16/F10 cells. Taken together, our data suggest that $P2X_7$ receptor mediates, at least in part, the antiproliferation action of ATP in B16 melanoma cells.
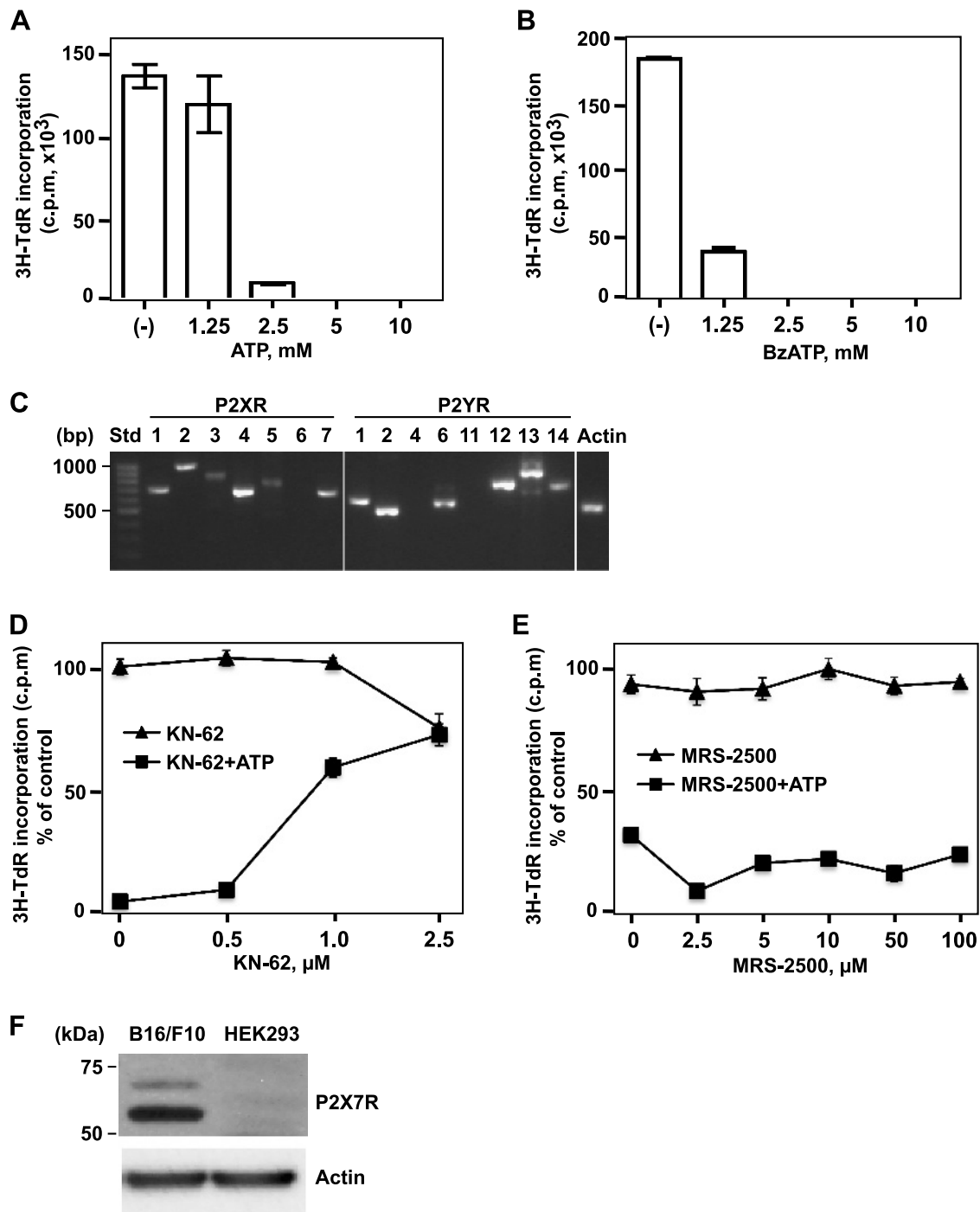
Figure 1. Antiproliferative effects of ATP on B16 melanoma cells are mediated through the P2X$_7$ receptor. High levels of extracellular ATP and BzATP inhibited melanoma cell proliferation in a dose-dependent manner. (A and B) Luc-B16/F10 cells were treated with ATP (A) or BzATP (B) at the indicated concentrations for 16 hours, and cell proliferation was determined by ^{3}H-TdR incorporation assay. Columns indicate mean of triplicate determinations; bars, SD. (C) mRNA expression of P2 receptors in luc-B16/F10 cells were determined by RT-PCR. The PCR products were visualized by agarose gel electrophoresis. The size standards (Std) are shown in the left lane. (D and E) Luc-B16/F10 cells were exposed to antagonists of P2Rs (KN-62, selective for P2X$_7$; MRS-2500, selective for P2Y$_1$), at indicated concentrations, in the presence or absence of ATP (2.5 mM) for 16 hours. Cell proliferation was assessed by ^{3}H-TdR incorporation and indicated as a percentage of untreated control cells. Points indicate mean of triplicate determinations; bars, SD. (F) Immunoblot analysis of the P2X$_7$ expression in luc-B16/F10 cells. A sample of total cell lysates (20 μg of protein) from luc-B16/F10 cells was run in parallel with a sample of HEK293 cell lysates (20 μg, negative control) and probed with P2X$_7$ antibody (top). β-Actin was used as loading control (bottom). Size standards are shown in the left lane.

ATP Promotes Tumor Cell Death through P2X₇ Receptor

Besides inhibition of cell proliferation, other mechanisms for antitumor function of ATP include direct induction of cell death. Dramatic decreases in cell growth caused by ATP may be also associated with cell death. We next examined the cell death after ATP exposure (Figure 2). ATP induced cytotoxicity on melanoma cells (Figure 2*A*). *In situ* cellular analysis demonstrated that melanoma cell death (Fig-

ure 2, *B-D*) with decreases in cell confluency and cell count was triggered on ATP stimulation, in a dose-dependent manner.

Similar effects were observed in MCA38 colon cancer cells albeit with different sensitivity to ATP (Figure W2 and data not shown), in keeping with data shown in Figure W1.

To precisely examine patterns of apoptosis and necrosis in the setting of ATP-induced cell death, the staining pattern of the cells were
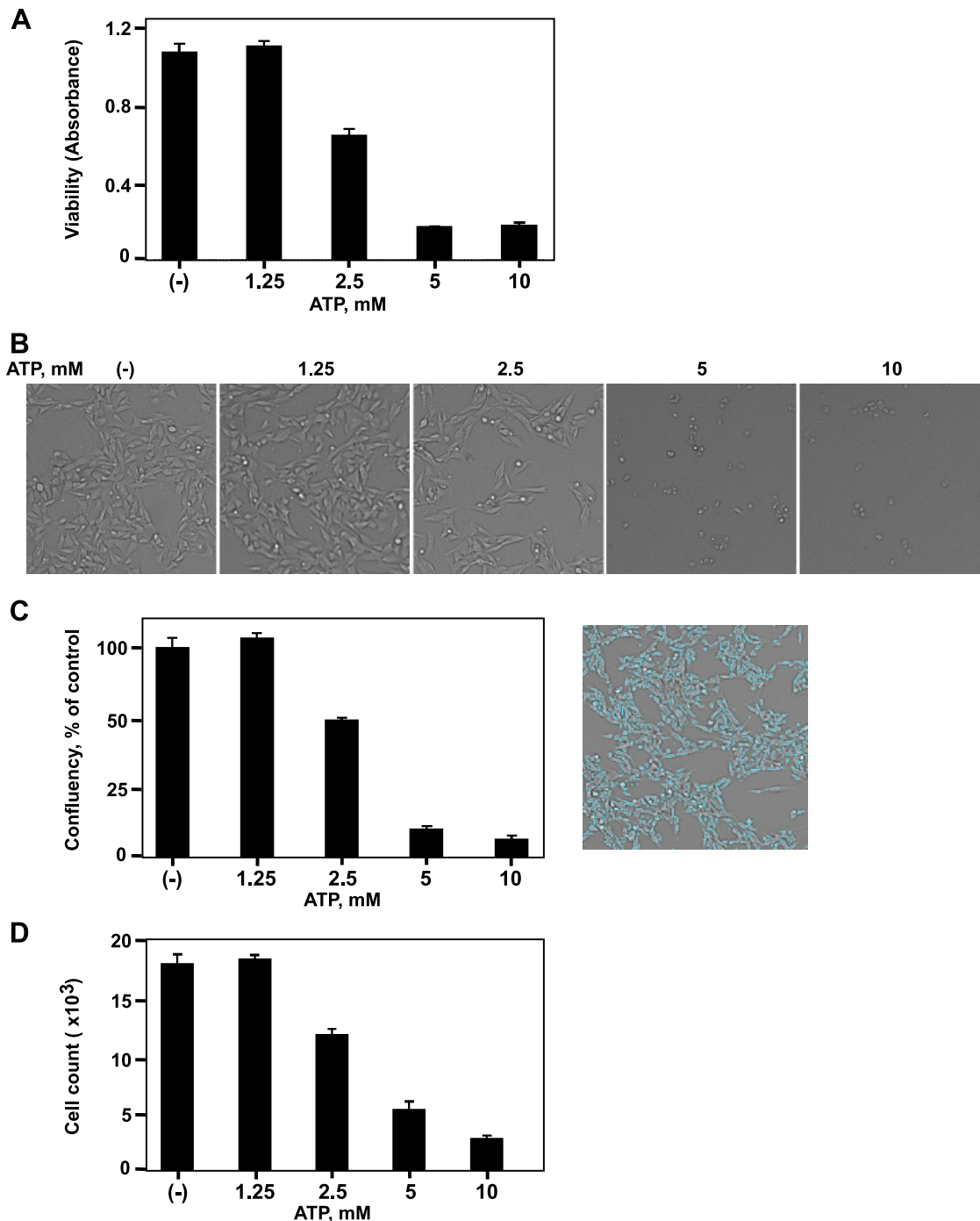

Figure 2. ATP-induced B16 melanoma cell death. Luc-B16/F10 cells were treated with ATP at the indicated concentrations for 16 hours. (A) Cell viability was measured using Cell Counting Kit-8. Cells were also imaged and counted using the Celigo Cell Counting application. (B) Representative brightfield images of live luc-B16/F10 cells. (C) Confluency of cells per well is expressed as a percentage of untreated control cells (left). Representative image of control cells with gating of confluency is shown on the right. (D) Cell count per well. Columns indicate mean of triplicate determinations; bars, SD.

analyzed with fluorescein isothiocyanate (FITC)–conjugated annexin V and PI by flow cytometry [35,36]. In this experiment, luc-B16/F10 cells treated with ATP (2.5 mM) alone or together with KN-62 (2.5 μM), or MRS-2500 (2.5 μM), or suramin (250 μM) were stained simultaneously with both FITC–annexin V and PI. Induction of both apoptosis and necrosis were observed in cells exposed to ATP in a time-dependent manner (Figure 3A, top). In addition, ATP-stimulated apoptotic/necrotic cell death could be blocked by coincubation with a P2X$_7$ antagonist, KN-62 (2.5 μM; Figure 3A, bottom), but not by coincubation of MRS-2500 or suramin (data not shown).

Next, we tested the cleavage of caspase-3 and caspase-9 as markers of apoptosis. Figure 3B showed that the levels of cleaved caspase-3 (Figure 3B, top), and caspase-9 (Figure 3B, bottom) increased over time after exposure to ATP. These observations were further confirmed by Western blot analysis using anti–cleaved caspase-3 and caspase-9 antibodies (Figure 3C, left). Furthermore, coincubation of cells with KN-62 (2.5 μM) blocked ATP-induced cleavage of caspase-3 and caspase-9 (Figure 3C, right).

Quantitative real-time PCR revealed that treatment with ATP (2.5 mM) for 16 hours significantly increased the mRNA expression level of P2X$_7$, whereas cotreatment with KN-62 (2.5 μM) abrogated the increase in P2X$_7$ expression (Figure 3D). These findings indicate that ATP-induced cell death in B16 melanoma cells is associated with both apoptosis and necrosis and is at least partly mediated through the P2X$_7$ receptor.

Apyrase (Soluble NTPDase) or Vascular Cell CD39 Expressed by LSECs Abrogates/Reverses Antitumor Activity of ATP

Next, we sought to determine whether scavenging of extracellular ATP by apyrase, a soluble form of NTPDase with ATPase and ADPase activity at a 1:1 ratio, could rescue ATP-stimulated growth inhibition of tumor cells. Figure 4A showed that tumor cell growth inhibition triggered by ATP (2.5 mM) was completely abrogated by coincubation of cells with apyrase (10 U/ml). The rescue of tumor cells by apyrase was dose dependent.

CD39 and CD73 are the major ectonucleotidases expressed by LSECs. Next, LSECs were purified from wt, Cd39 null, or Cd73 null livers and were cocultured with luc-B16/F10 cells for 24 hours, at various ratios of cell numbers, before being exposed to ATP (2.5 mM) for 16 hours.

Successful isolation of healthy LSECs was verified by uptake of DiI-labeled Ac-LDL and FACS analysis for endothelium makers (including CD31, CD34, and Flk-1) (data not shown), as established previously [31,32].

As shown in Figure 4B, wt LSECs attenuated the inhibitory effects of ATP on tumor cell growth, whereas Cd39 null LSECs did not retain this capacity. Interestingly, growth inhibition by ATP was reversed by Cd73 null LSECs to a greater extent, when compared with wt LSECs (Figure 4B). The rescue observed with wt and Cd73 null LSECs was dose dependent.

We also noted that extracellular ATP inhibited growth of LSECs (Figure W3 for wt cells and data not shown for null cells).

To further investigate the mechanisms underlying the observations in Figure 4B, purine metabolism by ectonucleotidase activity of freshly isolated LSECs was examined by TLC analysis using ADP-C^{14} as substrate. ADP was first hydrolyzed to AMP and then to adenosine by wt LSECs. Adenosine was further degraded to hypoxanthine by wt LSECs (Figure 4C). Cd73 null LSECs could only generate AMP but not adenosine (Figure 4C). Cd39 null LSECs and luc-B16/F10

cells had minimal nonspecific ectonucleotidase activity, in contrast to wt LSECs (Figure 4C). These findings clearly explain how wt, Cd73 null, and Cd39 null LSECs exhibit differential salvage abilities on ATP-induced growth inhibition as observed in Figure 4B.

Defective Angiogenesis Is Associated with Heightened Tumor Necrosis and Increased P2X$_7$ Expression in Cd39 Null Tumor-Bearing Mice

We next determined whether injured tumor cells could release endogenous mediators that directly result in cellular damage of contiguous/adjacent tumor cells. Luc-B16/F10 cells were injected (s.c.) into flanks of wild type C57BL/6 mice for 14 days, tumors were excised, and tumor supernatants were prepared (see Materials and Methods), these were then added to luc-B16/F10 cell cultures. In Figure 5A, we show that melanoma cell proliferation was inhibited by the addition of tumor supernatants in a concentration-dependent manner. Dramatic increases in ATP levels were also noted in these tumor supernatants compared with the prewash media (Figure W4). However, coincubation with apyrase alone failed to rescue the growth inhibitory effects triggered by these crude tumor supernatants (data not shown) as previously noted with exogenous ATP (Figure 4A). These data suggest that other cytotoxic constituents besides nucleotides contribute to the tumor killing activity of supernatants.

We have recently demonstrated the effect of Cd39 deletion on melanoma growth in vivo using a murine model of hepatic metastases of B16/F10 melanoma [21]. We noted that immune cell as well as vascular CD39 expression promote tumor growth, whereas pharmacological inhibition of CD39 enzymatic activity (in contrast) abrogates tumor growth [21].

We stained these liver tumor sections using anti-CD31 (a marker for endothelium) and anti-CD39 antibodies. We observed that CD39 was expressed on tumor-associated endothelial cells (ECs) in wt livers. In contrast, in Cd39 null tumor-bearing livers, lack of CD39 expression (suggesting decreased ATP scavenging in the tumor microenvironment) was associated with defective angiogenesis and larger areas of necrosis within the centers of tumors (Figure 5B). Immunofluorescent staining on tumor sections further showed that protein expression of P2X$_7$ was increased on melanoma cells in Cd39 null tumor-bearing livers compared with wt livers (Figure 5C).

Discussion

The present study clearly demonstrates that tumor-derived mediators, inclusive of ATP, directly exert growth inhibitory effects on tumor cells. The P2X$_7$ receptor is functionally expressed in B16/F10 melanoma cells and is responsible, at least in part, for such ATP-induced growth inhibition and cell death. Importantly, coculture of tumor cells with LSECs demonstrates that expression of ecto-enzyme CD39 by endothelial cells counteracts tumoricidal actions stimulated by extracellular ATP. Collectively, in light of ATP-induced tumor suppression, our results indicate novel purinergic mechanisms implicated in tumor biology: 1) danger signals (including ATP) released by necrotic tumor cells result in subsequent death of neighboring tumor cells and 2) CD39 expressed on ECs promotes tumor cell growth by scavenging extracellular ATP in the tumor microenvironment.

Different P2 receptor subtypes have been shown to modulate different cellular functions such as proliferation, differentiation, and apoptosis. P2Y$_1$ and P2X$_7$ receptors are expressed in human melanoma cells in situ and mediate apoptotic and necrotic actions of ATP [38].

The antitumor actions of these receptors contain three processes: inhibition of cell proliferation, promotion of cell differentiation (resulting in inhibition of cell proliferation), and cell death [2]. Here, we show that antitumor activity of ATP is largely due to the combination of inhibition of cell proliferation and induction of cell death.

These two processes are both mediated largely through the expression of P2X$_7$.

When ATP appears in the extracellular space of tumor microenvironment, this mediator is rapidly hydrolyzed by ectonucleotidases to ADP, AMP, and, finally, adenosine [12]. Most studies to date
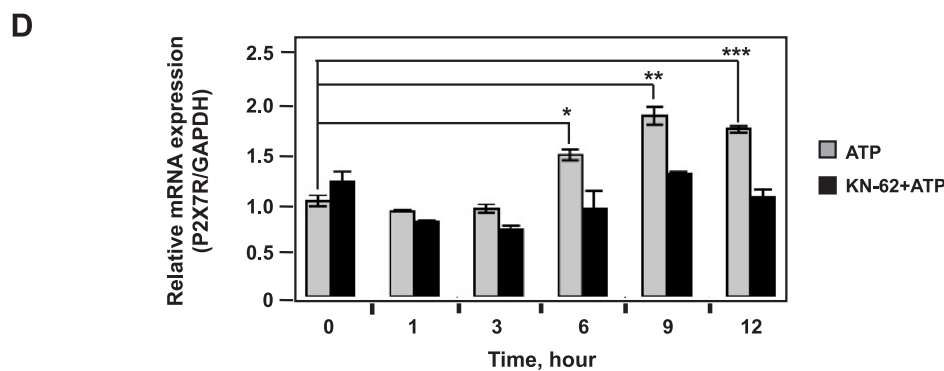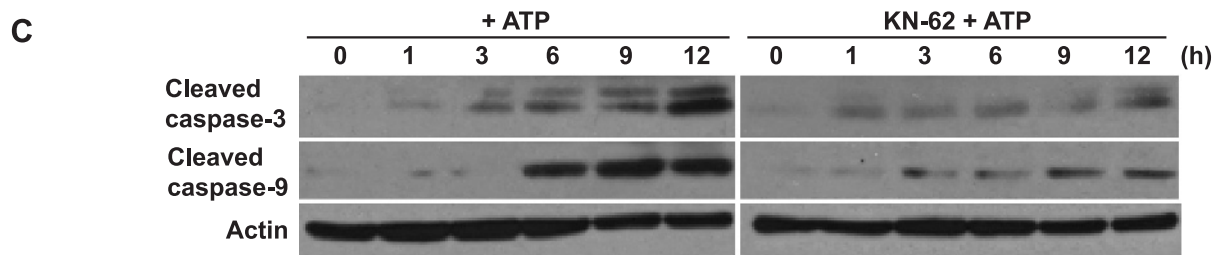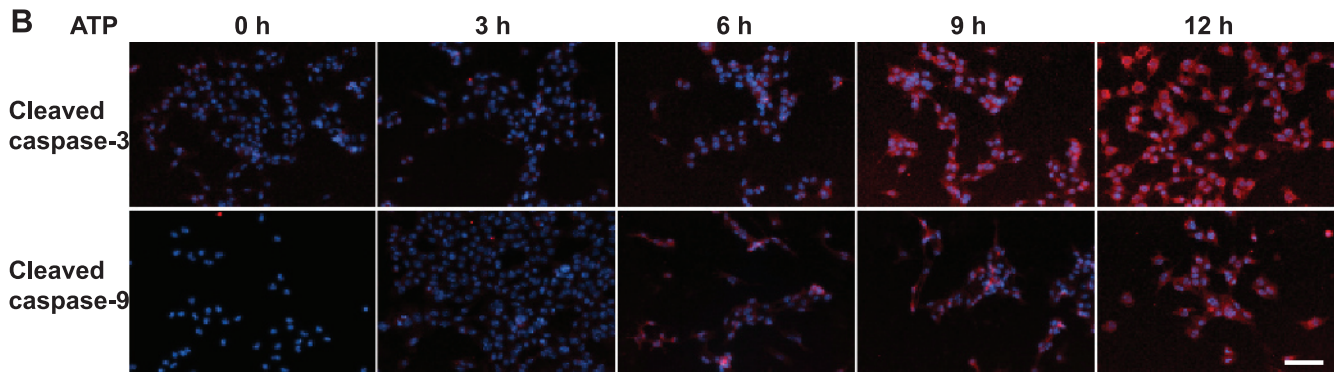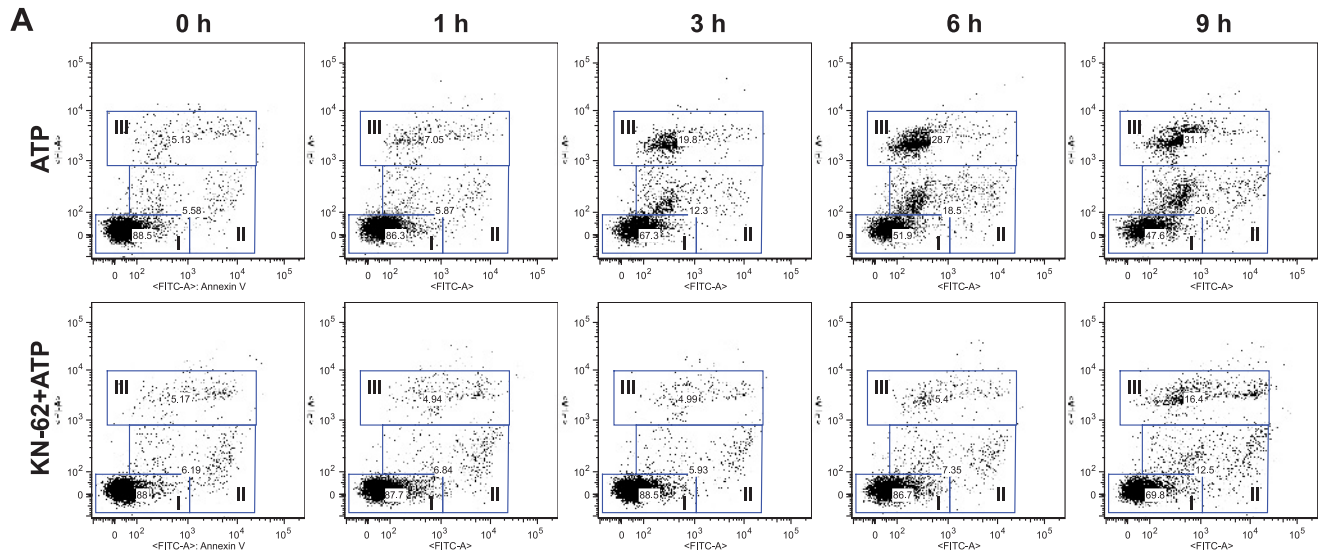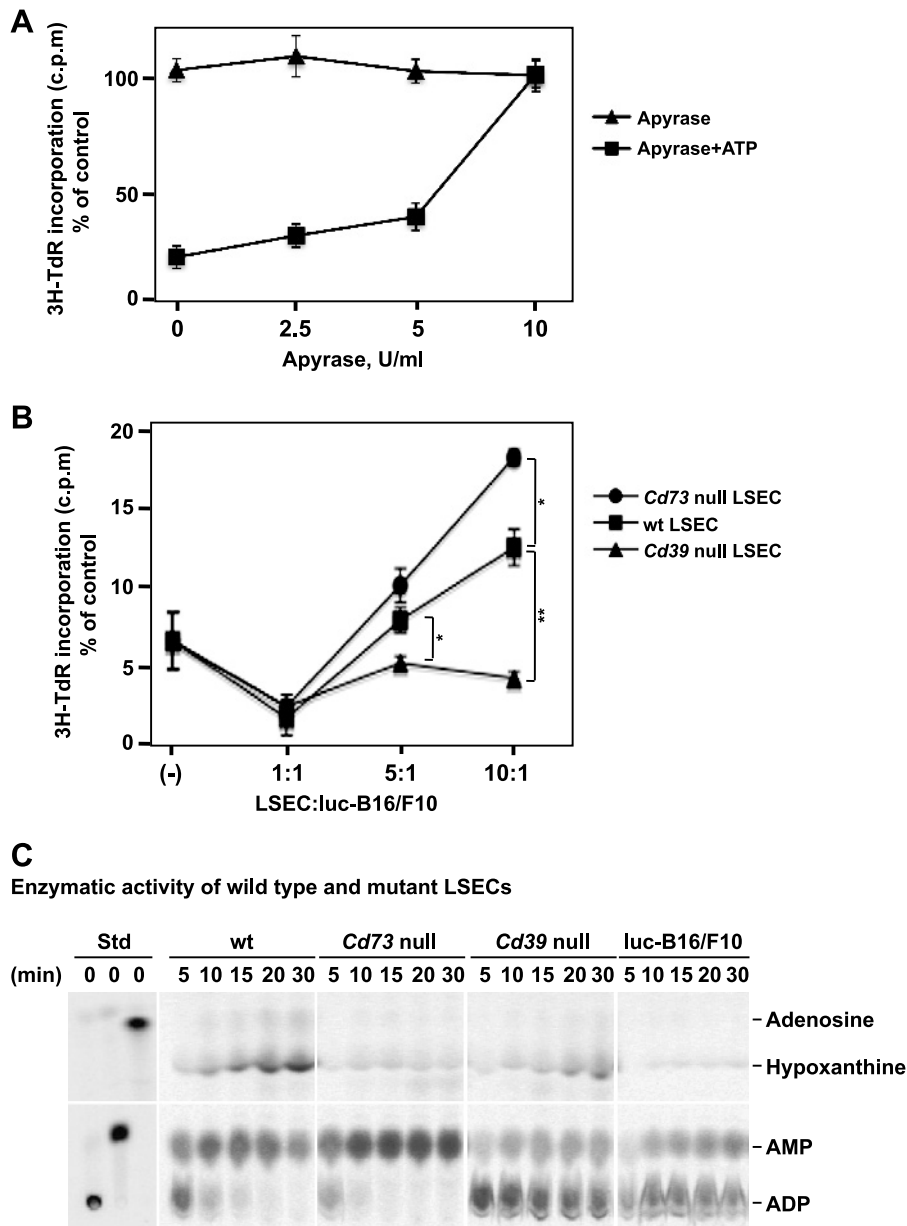
Figure 4. Apyrase (soluble NTPDase) or CD39 expression on LSECs abrogates the inhibitory effects of ATP on B16 melanoma cell growth. (A) Inhibitory effects of ATP are alleviated by addition of apyrase. Luc-B16/F10 cells were treated with apyrase at indicated concentrations for 30 minutes and then exposed to ATP (2.5 mM). Sixteen hours later, cell proliferation was analyzed by ^{3}H-TdR incorporation assay and expressed as a percentage of untreated control cells. Points indicate mean of triplicate determinations; bars, SD. (B) LSECs were isolated from C57BL/6 wild type (wt), *Cd39* null, and *Cd73* null mice and were cocultured with Luc-B16/F10 cells (3×10^5) at the indicated ratios of cell numbers for 24 hours before being exposed to ATP (2.5 mM). Cell proliferation was assayed and expressed as a percentage of untreated control cells. Points indicate mean of triplicate determinations; bars, SD. *$P < .05$, **$P = .002$. (C) Freshly purified LSECs or luc-B16/F10 cells (3×10^5 cells per cell type) were subjected to TLC analysis for assessment of NTPDase activity. [C^{14}]ADP, [C^{14}]AMP, and [C^{14}]ADO incubated in PBS served as standards.

Figure 3. ATP-induced apoptosis/necrosis of B16 melanoma cells is mediated through P2X$_7$ receptor. Time course of ATP-induced cell death in luc-B16/F10 cells is shown. The cells were exposed to 2.5 mM of ATP or in combination with KN-62 (2.5 μM) for the indicated periods. (A) Time course of ATP-induced apoptosis and necrosis of luc-B16/F10 cells. FITC–Annexin V/PI staining of luc-B16/F10 cells was assessed by flow cytometry at indicated times. The gates are defined as follows: I (lower left), viable; II (middle), apoptotic; and III (upper), necrotic. (B) Cells were fixed and stained with anti–cleaved caspase-3 or caspase-9 antibodies. Cleaved caspase-3 and caspase-9 were visualized by fluorescent microscopy. Representative images for each time point. Scale bar, 100 μm. The cleavage of caspase-3 and caspase-9 (red) were elevated in the cytoplasm as well as in the nuclei (blue, Hoechst dye 33258) in a time-dependent manner. (C) Cells were harvested, lysed, and used for immunoblot analysis of cleavage of caspase-3 (top) and caspase-9 (middle). Twenty micrograms of protein was loaded per lane, and gel loading was normalized by β-actin (bottom). (D) RQ-PCR analysis of P2X$_7$ mRNA expression in luc-B16/F10 cells after treatment. Columns indicate mean of triplicate determinations; bars, SD. *$P = .01$, **$P = .001$, ***$P = .002$.

have focused on the alterations of purinergic receptors in tumors, whereas ectonucleotidases are much less investigated. Purinergic signaling can be modulated by modifying the expression and/or activity of these ectoenzymes in addition to changes in P2 receptor levels [11,40].

Figure 5. Metastatic melanoma growth in *Cd39* null mice. (A) Dose-dependent inhibitory effects of tumor supernatants (16 hours of treatment) on luc-B16/F10 melanoma cell proliferation. (B) Representative immunohistochemical staining on tumor tissue sections obtained from melanoma metastasized to mouse livers using anti-CD31 (a marker for endothelium) and anti-CD39 antibodies and TUNEL staining (TdT) for apoptosis. (C) P2X$_7$ expression on tumor tissues. Representative fluorescence immunohistochemical staining using anti-P2X$_7$ antibody: Hoechst dye 33258 staining nuclei in blue and P2X$_7$ in red. Columns indicate mean of triplicate determinations; bars, SD. Scale bar, 100 μm.

This study shows for the first time that deletion of *Cd39* on ECs enhances antitumor activity of ATP, whereas deletion of *Cd73* on ECs has different effects. These data suggest a feasible approach to augment anticancer therapy by modulating expression and/or enzymatic activity of NTPDase-type ectonucleotidases. This approach might be easier to achieve and more efficacious than to independently target several purinergic receptors.

CD39 is also expressed by immune cells inclusive of Treg (CD4$^+$ Foxp3$^+$) and memory cells (CD4$^+$CD44$^+$CD62L$^-$Foxp3$^-$) [21,41]. These cells often infiltrate into solid tumors [21]. Whether these CD39$^+$ infiltrating immune cell populations also contribute to degradation of cytotoxic ATP in the tumor microenvironment and thereby independently promote tumor growth remains unclear.

Exposure of ECs to elevated levels of ATP has been shown to promote apoptosis *in vitro* [42]. We have previously demonstrated that inhibition of tumor growth in *Cd39* null mice is associated with defects of tumor angiogenesis [20,21]. Moreover, in this study, we show that ATP also exhibits direct growth inhibitory effects on LSECs (Figure W3 and data not shown) that further compromises cell-associated NTPDase activity. Therefore, the reduction of tumor size and volume in *Cd39* null tumor-bearing mice might result from dual actions of ATP on tumor cells as well as on ECs.

The phosphohydrolysis of ATP to adenosine has a complex modulatory effect on tumor cell proliferation and growth [43–45]. Adenosine ultimately derived from ATP may be responsible for some of the observed effects as this nucleoside has been shown to affect tumor growth in a cell-specific manner determined by concentrations and kinetics of exposure [43–45] (and unpublished observations in our laboratory). Tumor cell expressions of A2A and A2B have been shown to be proapoptotic and have antitumor activity [44,45]. The actions of A3 are contradictory. Most studies have demonstrated that A3 agonists induce apoptosis and tumor growth inhibition [45–48], whereas others show that A3 stimulation blocks A2A-induced cell death and ensures cell survival [43].

Therefore, the ambient vascular nucleotide/nucleoside milieu as regulated by ectonucleotidases and ectonucleotidases dictates the efficacy of antitumor activity of ATP *in vivo*. In this study, the differential salvage abilities on ATP-triggered tumor cell growth inhibition and NTPDase activity exhibited by wt, *Cd73* null, and *Cd39* null LSECs (Figure 4, *B* and *C*) are indicative of the participation of ATP-derived adenosine in the antitumor function of ATP.

Dzhandzhugazyan et al. [49] have shown that CD39 is the major ectonucleotidase in human melanocytes and melanoma cell lines and CD39 is overexpressed in differentiated human melanomas. It has been recently reported that CD73 is expressed on various tumor cells (e.g., ID8 ovarian cancer cells) and participates in adenosine generation, thereby suppressing antitumor immune responses [50], but potentially also affecting cancer cell apoptosis.

We therefore also examined the expression of CD39 and CD73 on tumor cells used for this study. Neither CD39 nor CD73 expression was observed on cultured B16/F10 or MCA38 cells as well as on malignant cells in metastatic tumors in the livers and lungs at any progression stage after tumor challenge [20,21] (data not shown).

Lastly, we have also shown that ATP exhibits cytotoxic effects on MCA38 colon cancer cells as well, suggesting general feature of antitumor capability of ATP (Figures W1 and W2; data not shown).

In summary, we postulate an intriguing mechanism by which extracellular ATP released by dying tumor cells accumulates to high concentrations that not only function as danger signals to the im-
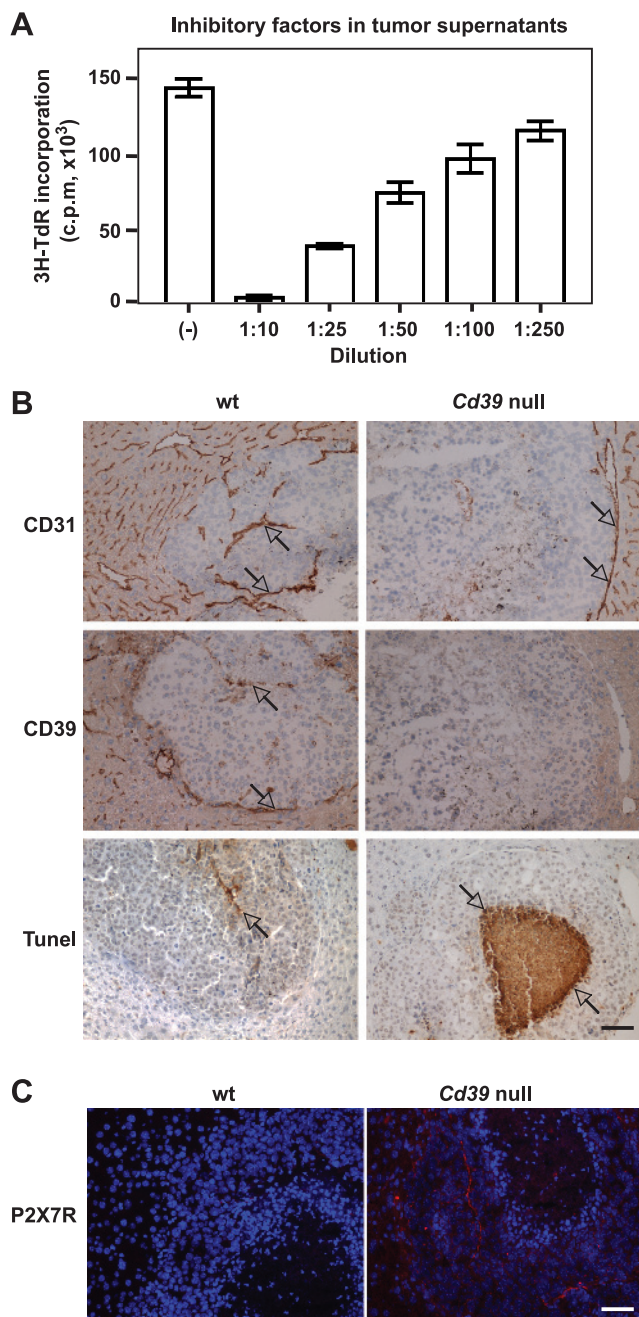
mune system but also can directly kill adjacent tumor cells. Our data showing that the antitumor activities of ATP are dose-dependent and can be amplified by inhibition of ectonucleotidase, such as CD39, open new avenues for investigation in cancer management.

Acknowledgments

References

[1] Burnstock G and Knight GE (2004). Cellular distribution and functions of P2 receptor subtypes in different systems. *Int Rev Cytol* **240**, 31–304.

[2] Shabbir M and Burnstock G (2009). Purinergic receptor–mediated effects of adenosine 5′-triphosphate in urological malignant diseases. *Int J Urol* **16**, 143–150.

[3] Burnstock G (2006). Purinergic P2 receptors as targets for novel analgesics. *Pharmacol Ther* **110**, 433–454.

[4] Burnstock G and Kennedy C (1985). Is there a basis for distinguishing two types of P2-purinoceptor? *Gen Pharmacol* **16**, 433–440.

[5] Burnstock G (2006). Purinergic signalling—an overview. *Novartis Found Symp* **276**, 26–48; discussion 48–57, 275–281.

[6] Burnstock G (2007). Purine and pyrimidine receptors. *Cell Mol Life Sci* **64**, 1471–1483.

[7] Rapaport E (1983). Treatment of human tumor cells with ADP or ATP yields arrest of growth in the S phase of the cell cycle. *J Cell Physiol* **114**, 279–283.

[8] Rapaport E (1988). Experimental cancer therapy in mice by adenine nucleotides. *Eur J Cancer Clin Oncol* **24**, 1491–1497.

[9] White N and Burnstock G (2006). P2 receptors and cancer. *Trends Pharmacol Sci* **27**, 211–217.

[10] Shabbir M, Thompson C, Jarmulowiczc M, Mikhailidis D, and Burnstock G (2008). Effect of extracellular ATP on the growth of hormone-refractory prostate cancer *in vivo*. *BJU Int* **102**, 108–112.

[11] Deli T and Csernoch L (2008). Extracellular ATP and cancer: an overview with special reference to P2 purinergic receptors. *Pathol Oncol Res* **14**, 219–231.

[12] Zimmermann H (2000). Extracellular metabolism of ATP and other nucleotides. *Naunyn Schmiedebergs Arch Pharmacol* **362**, 299–309.

[13] Trautmann A (2009). Extracellular ATP in the immune system: more than just a "danger signal". *Sci Signal* **2**, pe6.

[14] Behrens MD, Wagner WM, Krco CJ, Erskine CL, Kalli KR, Krempski J, Gad EA, Disis ML, and Knutson KL (2008). The endogenous danger signal, crystalline uric acid, signals for enhanced antibody immunity. *Blood* **111**, 1472–1479.

[15] Apetoh L, Ghiringhelli F, Tesniere A, Obeid M, Ortiz C, Criollo A, Mignot G, Maiuri MC, Ullrich E, Saulnier P, et al. (2007). Toll-like receptor 4–dependent contribution of the immune system to anticancer chemotherapy and radiotherapy. *Nat Med* **13**, 1050–1059.

[16] Mariathasan S, Weiss DS, Newton K, McBride J, O'Rourke K, Roose-Girma M, Lee WP, Weinrauch Y, Monack DM, and Dixit VM (2006). Cryopyrin activates the inflammasome in response to toxins and ATP. *Nature* **440**, 228–232.

[17] Martins I, Tesniere A, Kepp O, Michaud M, Schlemmer F, Senovilla L, Seror C, Metivier D, Perfettini JL, Zitvogel L, et al. (2009). Chemotherapy induces ATP release from tumor cells. *Cell Cycle* **8**, 3723–3728.

[18] Aymeric L, Apetoh L, Ghiringhelli F, Tesniere A, Martins I, Kroemer G, Smyth MJ, and Zitvogel L (2010). Tumor cell death and ATP release prime dendritic cells and efficient anticancer immunity. *Cancer Res* **70**, 855–858.

[19] Ghiringhelli F, Apetoh L, Tesniere A, Aymeric L, Ma Y, Ortiz C, Vermaelen K, Panaretakis T, Mignot G, Ullrich E, et al. (2009). Activation of the NLRP3 inflammasome in dendritic cells induces IL-1β–dependent adaptive immunity against tumors. *Nat Med* **15**, 1170–1178.

[20] Jackson SW, Hoshi T, Wu Y, Sun X, Enjyoji K, Cszimadia E, Sundberg C, and Robson SC (2007). Disordered purinergic signaling inhibits pathological angiogenesis in cd39/Entpd1-null mice. *Am J Pathol* **171**, 1395–1404.

[21] Sun X, Wu Y, Gao W, Enjyoji K, Csizmadia E, Muller CE, Murakami T, and Robson SC (2010). CD39/ENTPD1 expression by CD4+Foxp3+ regulatory T cells promotes hepatic metastatic tumor growth in mice. *Gastroenterology* **139**(3), 1030–1040.

[22] Plesner L (1995). Ecto-ATPases: identities and functions. *Int Rev Cytol* **158**, 141–214.

[23] Enjyoji K, Sevigny J, Lin Y, Frenette PS, Christie PD, Esch JS II, Imai M, Edelberg JM, Rayburn H, Lech M, et al. (1999). Targeted disruption of cd39/ATP diphosphohydrolase results in disordered hemostasis and thromboregulation. *Nat Med* **5**, 1010–1017.

[24] Robson SC, Wu Y, Sun X, Knosalla C, Dwyer K, and Enjyoji K (2005). Ecto-nucleotidases of CD39 family modulate vascular inflammation and thrombosis in transplantation. *Semin Thromb Hemost* **31**, 217–233.

[25] Mills JH, Thompson LF, Mueller C, Waickman AT, Jalkanen S, Niemela J, Airas L, and Bynoe MS (2008). CD73 is required for efficient entry of lymphocytes into the central nervous system during experimental autoimmune encephalomyelitis. *Proc Natl Acad Sci USA* **105**, 9325–9330.

[26] Sato A, Ohtsuki M, Hata M, Kobayashi E, and Murakami T (2006). Antitumor activity of IFN-λ in murine tumor models. *J Immunol* **176**, 7686–7694.

[27] Jun DJ, Kim J, Jung SY, Song R, Noh JH, Park YS, Ryu SH, Kim JH, Kong YY, Chung JM, et al. (2007). Extracellular ATP mediates necrotic cell swelling in SN4741 dopaminergic neurons through P2X$_7$ receptors. *J Biol Chem* **282**, 37350–37358.

[28] Kunzli BM, Nuhn P, Enjyoji K, Banz Y, Smith RN, Csizmadia E, Schuppan D, Berberat PO, Friess H, and Robson SC (2008). Disordered pancreatic inflammatory responses and inhibition of fibrosis in CD39-null mice. *Gastroenterology* **134**, 292–305.

[29] Kaczmarek E, Koziak K, Sevigny J, Siegel JB, Anrather J, Beaudoin AR, Bach FH, and Robson SC (1996). Identification and characterization of CD39/vascular ATP diphosphohydrolase. *J Biol Chem* **271**, 33116–33122.

[30] Deaglio S, Dwyer KM, Gao W, Friedman D, Usheva A, Erat A, Chen JF, Enjyoji K, Linden J, Oukka M, et al. (2007). Adenosine generation catalyzed by CD39 and CD73 expressed on regulatory T cells mediates immune suppression. *J Exp Med* **204**, 1257–1265.

[31] LeCouter J, Moritz DR, Li B, Phillips GL, Liang XH, Gerber HP, Hillan KJ, and Ferrara N (2003). Angiogenesis-independent endothelial protection of liver: role of VEGFR-1. *Science* **299**, 890–893.

[32] Beldi G, Wu Y, Sun X, Imai M, Enjyoji K, Csizmadia E, Candinas D, Erb L, and Robson SC (2008). Regulated catalysis of extracellular nucleotides by vascular CD39/ENTPD1 is required for liver regeneration. *Gastroenterology* **135**, 1751–1760.

[33] Wu Y, Sun X, Kaczmarek E, Dwyer KM, Bianchi E, Usheva A, and Robson SC (2006). RanBPM associates with CD39 and modulates ecto-nucleotidase activity. *Biochem J* **396**, 23–30.

[34] Beldi G, Wu Y, Banz Y, Nowak M, Miller L, Enjyoji K, Haschemi A, Yegutkin GG, Candinas D, Exley M, et al. (2008). Natural killer T cell dysfunction in CD39-null mice protects against concanavalin A–induced hepatitis. *Hepatology* **48**, 841–852.

[35] Koopman G, Reutelingsperger CP, Kuijten GA, Keehnen RM, Pals ST, and van Oers MH (1994). Annexin V for flow cytometric detection of phosphatidylserine expression on B cells undergoing apoptosis. *Blood* **84**, 1415–1420.

[36] Vermes I, Haanen C, Steffens-Nakken H, and Reutelingsperger C (1995). A novel assay for apoptosis. Flow cytometric detection of phosphatidylserine expression on early apoptotic cells using fluorescein labelled annexin V. *J Immunol Methods* **184**, 39–51.

[37] Goepfert C, Sundberg C, Sevigny J, Enjyoji K, Hoshi T, Csizmadia E, and Robson S (2001). Disordered cellular migration and angiogenesis in CD39-null mice. *Circulation* **104**, 3109–3115.

[38] White N, Knight GE, Butler PE, and Burnstock G (2009). An *in vivo* model of melanoma: treatment with ATP. *Purinergic Signal* **5**, 327–333.

[39] Humphreys BD, Virginio C, Surprenant A, Rice J, and Dubyak GR (1998). Isoquinolines as antagonists of the P2X7 nucleotide receptor: high selectivity for the human *versus* rat receptor homologues. *Mol Pharmacol* **54**, 22–32.

[40] Fang WG, Pirnia F, Bang YJ, Myers CE, and Trepel JB (1992). P2-purinergic receptor agonists inhibit the growth of androgen-independent prostate carcinoma cells. *J Clin Invest* **89**, 191–196.

[41] Zhou Q, Yan J, Putheti P, Wu Y, Sun X, Toxavidis V, Tigges J, Kassam N, Enjyoji K, Robson SC, et al. (2009). Isolated CD39 expression on CD4+ T cells denotes both regulatory and memory populations. *Am J Transplant* **9**, 2303–2311.

[42] Goepfert C, Imai M, Brouard S, Csizmadia E, Kaczmarek E, and Robson SC (2000). CD39 modulates endothelial cell activation and apoptosis. *Mol Med* **6**, 591–603.

[43] Merighi S, Mirandola P, Milani D, Varani K, Gessi S, Klotz KN, Leung E, Baraldi PG, and Borea PA (2002). Adenosine receptors as mediators of both

cell proliferation and cell death of cultured human melanoma cells. *J Invest Dermatol* **119**, 923–933.

[44] Merighi S, Mirandola P, Varani K, Gessi S, Leung E, Baraldi PG, Tabrizi MA, and Borea PA (2003). A glance at adenosine receptors: novel target for anti-tumor therapy. *Pharmacol Ther* **100**, 31–48.

[45] Panjehpour M and Karami-Tehrani F (2007). Adenosine modulates cell growth in the human breast cancer cells via adenosine receptors. *Oncol Res* **16**, 575–585.

[46] Kim SJ, Min HY, Chung HJ, Park EJ, Hong JY, Kang YJ, Shin DH, Jeong LS, and Lee SK (2008). Inhibition of cell proliferation through cell cycle arrest and apoptosis by thio-Cl-IB-MECA, a novel A3 adenosine receptor agonist, in human lung cancer cells. *Cancer Lett* **264**, 309–315.

[47] Fishman P, Bar-Yehuda S, Madi L, and Cohn I (2002). A3 adenosine receptor as a target for cancer therapy. *Anticancer Drugs* **13**, 437–443.

[48] Fishman P, Bar-Yehuda S, Ohana G, Barer F, Ochaion A, Erlanger A, and Madi L (2004). An agonist to the A3 adenosine receptor inhibits colon carcinoma growth in mice via modulation of GSK-3 β and NF-κB. *Oncogene* **23**, 2465–2471.

[49] Dzhandzhugazyan KN, Kirkin AF, thor Straten P, and Zeuthen J (1998). Ecto-ATP diphosphohydrolase/CD39 is overexpressed in differentiated human melanomas. *FEBS Lett* **430**, 227–230.

[50] Jin D, Fan J, Wang L, Thompson LF, Liu A, Daniel BJ, Shin T, Curiel TJ, and Zhang B (2010). CD73 on tumor cells impairs antitumor T-cell responses: a novel mechanism of tumor-induced immune suppression. *Cancer Res* **70**, 2245–2255.

Table W1. RT-PCR Primers.

Transcript	Primer Sequence
Mouse P2X$_1$	Forward 5′-tcattgccagaggctttc-3′
	Reverse 5′-gtggagggttgtatgtgt-3′
Mouse P2X$_2$	Forward 5′-caaagcctatgggattcg-3′
	Reverse 5′-cctatgaggagttctgtt-3′
Mouse P2X$_3$	Forward 5′-gtgaaaagctggaccattgg-3′
	Reverse 5′-gctgccattctccatcttgt-3′
Mouse P2X$_4$	Forward 5′-tacgtcattgggtgggtgtt-3′
	Reverse 5′-cttgatctggatacccatga-3′
Mouse P2X$_5$	Forward 5′-aggacattgacacttccctg-3′
	Reverse 5′-catcaggtcacggaactcta-3′
Mouse P2X$_6$	Forward 5′-gtggtagtctacgtgatagg-3′
	Reverse 5′-gcctctctatccacatacag-3′
Mouse P2X$_7$	Forward 5′-cttgccaactatgaacgg-3′
	Reverse 5′-cttggcctttgccaactt-3′
Mouse P2Y$_1$	Forward 5′-ttatgtcagcgtgctggtgt-3′
	Reverse 5′-cgtgtctccattctgcttga-3′
Mouse P2Y$_2$	Forward 5′-gaggacttcaagtacgtgct-3′
	Reverse 5′-acggagctgtaagccacaaa-3′
Mouse P2Y$_4$	Forward 5′-aacaactgcttcctccct-3′
	Reverse 5′-aagtcctagaggtaggtg-3′
Mouse P2Y$_6$	Forward 5′-cctgatgtatgcctgttcac-3′
	Reverse 5′-cacagccaagtaggctgtct-3′
Human P2Y$_{11}$*	Forward 5′-tgtggcccatactggtggttgag-3′
	Reverse 5′-gaagaagggtgcacgatgccca-3′
Mouse P2Y$_{12}$	Forward 5′-atatgcctggtgtcaacacc-3′
	Reverse 5′-ggaatccgtgcaaagtggaa-3′
Mouse P2Y$_{13}$	Forward 5′-tgcagggcttcaacaagtct-3′
	Reverse 5′-cctttccccatctcacacat-3′
Mouse P2Y$_{14}$	Forward 5′-ggaacaccctgatcacaaag-3′
	Reverse 5′-tgaccttccgtctgactctt-3′
Mouse actin	Forward 5′-tgtacgtagccatccaggct-3′
	Reverse 5′-ggtaccaccagacaacactgt-3′

*Human P2Y$_{11}$ was used as a negative control as mouse cells do not express P2Y$_{11}$ receptor.
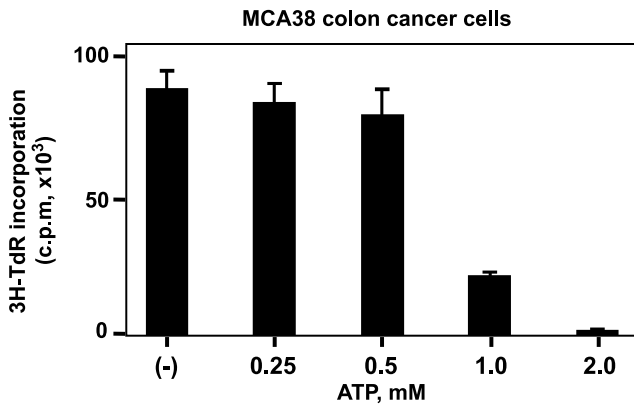

Figure W1. Effects of extracellular ATP on colon cancer cell proliferation. Extracellular ATP inhibited proliferation of colon cancer cells, in a dose-dependent manner. MCA38 cells were treated with ATP at the indicated concentrations for 16 hours. Cell proliferation was determined by ^{3}H-TdR incorporation assay. Columns indicate mean of triplicate determinations; bars, SD.
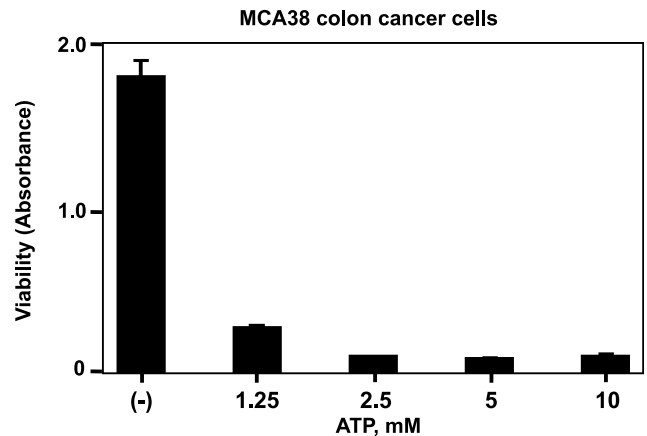

Figure W2. Effects of extracellular ATP on viability of colon cancer cells. Extracellular ATP exhibited cytotoxicity on colon cancer cells in a dose-dependent manner. MCA38 cells were treated with ATP at the indicated concentrations for 16 hours, and cell viability was evaluated using Cell Counting Kit-8. Columns indicate mean of triplicate determinations; bars, SD.
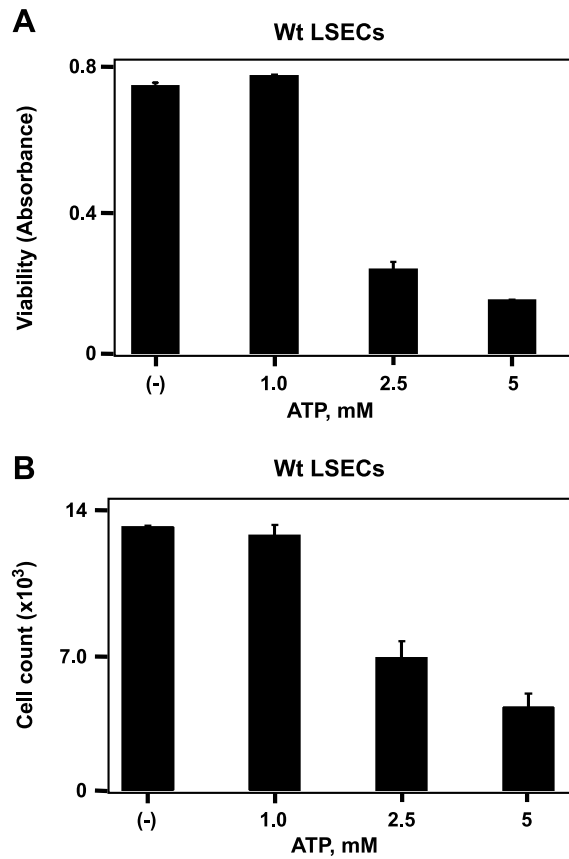
A

B

Figure W3. Effects of extracellular ATP on growth of wt LSECs. Extracellular ATP exhibited inhibitory effects on wt LSECs in a dose-dependent manner. Freshly purified wt LSECs were cultured for 24 hours before being exposed to ATP at the indicated concentrations for additional 16 hours. (A) Cell viability was evaluated using Cell Counting Kit-8. (B) Cells were counted using the Celigo Cell Counting application. Columns indicate mean of triplicate determinations; bars, SD.
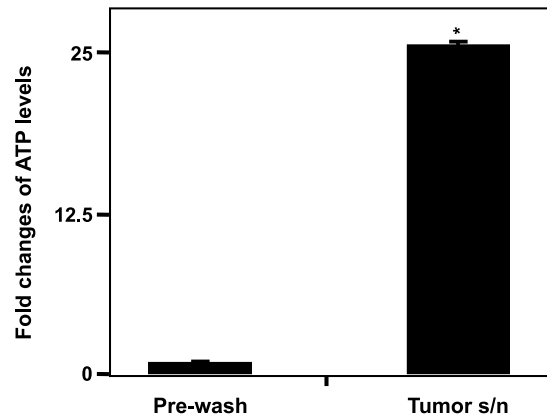

Figure W4. Release of ATP by damaged tumor cells. Extracellular ATP levels in prewash media (Pre-wash) and tumor supernatants (Tumor s/n) were measured using the ATP Colorimetric/Fluorometric Assay Kit (BioVision) and expressed as fold changes to the prewash medium. Columns indicate mean of triplicate determinations; bars, SD. *$P = 3.6e - 08$.